Evolutionary Biology (2023) 50:127–136
https://doi.org/10.1007/s11692-022-09593-x

RESEARCH ARTICLE

Opportunities and Constraints Imposed by the G matrix of *Drosophila buzzatii* Wings

P. P. Iglesias[1] · F. A. Machado[2] · S. Llanes[3] · E. Hasson[3] · E. M. Soto[3]

Received: 12 May 2022 / Accepted: 25 December 2022 / Published online: 10 January 2023

Abstract

The *Drosophila* wing is a structure shared by males and females with the primary function of flight. However, in males, wings are also used to produce songs or visual displays during courtship. Understanding the genetic architecture underlying wing variation within and between the sexes is central to predicting the possible outcomes of evolutionary pressures. Here, we investigate these issues by studying how the wing has evolved in twelve populations of *Drosophila buzzatii*, a species for which the courtship song is crucial to copulation. We found that females and males evolved in slightly different directions and that cross-sex covariances reduced the predicted response to selection in the direction of the extant sexual dimorphism. Moreover, we found evidence of directional selection consistent with the hypothesis of asymmetric selection acting on wing shape in each sex. In summary, the evolution of *D. buzzatii* wing shape seems to be the product of a complex interplay between genetic constraints due to between-sex pleiotropy, and conflicting selective pressures.

Keywords Genetic architecture · Intralocus sexual conflict · Multivariate selection · Sexual dimorphism · Wing shape

Introduction

To understand how complex phenotypes evolve under natural selection and random genetic drift, it is necessary to unveil the organization of the genetic variation underlying such traits (Lande, 1979; Steppan et al., 2002). Because of the complex nature of multicellular life, not all directions of the phenotypic space contain the same amount of variation, imposing limits and constraints on how populations might evolve (Arnold, 1992; Blows & Walsh, 2009; Futuyma, 2010). In the most extreme case, when such constraints are not aligned with the evolutionary forces acting on them, they can also impose demographic pressures that could lead to population decline (Lande, 1993; Burger & Lynch 1995; Chevin et al., 2010; Villmoare, 2013).

The G matrix is the main parameter in evolutionary genetics to understand populations and species' short and long-term evolutionary dynamics. The G matrix summarizes the available additive genetic variances and covariances among the multiple traits that comprise a phenotype. Such traits may not be fully independent if pleiotropy or linkage disequilibrium creates covariation among some or all of them (Falconer, 1996). The presence of genetic covariation among traits not only means that they will be inherited jointly, but also that selection on one of them will lead to an indirect response on the others (Lande, 1979). For sexually dimorphic species, this picture can be complicated further, as sexes might have a different distribution of genetic variation and be subject to different selective pressures (Sztepanacz & Houle, 2019). When phenotypes in both sexes rely on the same genetic architecture, they are most likely to be pleiotropically connected. Thus, the covariances among the traits expressed in different sexes may become an additional

P. P. Iglesias and F. A. Machado have contributed equally to this work.

✉ P. P. Iglesias
patricia.p.iglesias@gmail.com

✉ F. A. Machado
fmachado@okstate.edu

[1] Laboratorio de Genética Evolutiva, Universidad Nacional de Misiones and Instituto de Biología Subtropical – CONICET, Félix de Azara 1552, N3300LQH Misiones, Argentina

[2] Department of Integrative Biology, Oklahoma State University, Stillwater, USA

[3] Facultad de Ciencias Exactas y Naturales, Instituto de Ecología, Genética y Evolución de Buenos Aires (IEGEBA – CONICET), DEGE, Universidad de Buenos Aires, Buenos Aires, Argentina

source of constraint towards the evolution of divergent phenotypes (Sztepanacz & Houle, 2019).

Drosophila wings are an outstanding model for studying morphological variation since wing vein intersections allow us to define landmarks rigorously, which are the basis of modern geometric morphometrics. In *D. melanogaster*, wing shape has proved to be highly heritable and harbors additive genetic variation for almost all phenotypic dimensions in single-sex analyses (Houle & Meyer, 2015). However, when both sexes are considered, cross-sex covariances can reduce the effective dimensionality of the phenotype, limiting the independent response of the sexes to divergent selection (Sztepanacz & Houle, 2019).

Here, we investigated the variation of wing shape among populations and sexes, and the opportunities and constraints imposed by the G matrix in *D. buzzatii*.

Flies of this species allow us to properly address these issues since males and females use wings to fly, but only the males use wings to produce a courtship song, a trait that is crucial to copulation (Iglesias & Hasson, 2017; Iglesias et al., 2018a, 2018b). A previous study has shown that even though no population structure was found, male courtship song parameters diverged substantially among these populations (Iglesias et al., 2018b). Therefore, if wing morphology influences sound production, only male wings will be subject to sexual selection. As the male wing shape is probably a target for multiple selective pressures, we expected this sex to diverge more than females in their phenotype. Specifically, we ask: (i) Is there wing shape variation among populations and between sexes? (ii) Are cross-sex genetic covariances constraining wing shape dimorphism? (iii) Is there a signal of selection in females' and males' wings?

Materials and Methods

Data collection and measurements

We analyzed 12 populations of *D. buzzatii* flies previously used to study variation in male courtship songs (Iglesias et al., 2018b). Each population consisted of eight to 15 isofemale lines founded with wild-collected gravid females. Flies were raised under common-garden and controlled-density conditions (40 first-instar larvae per vial) and a photoperiod regimen of 12-h light: 12-h dark cycle. First, flies were raised on standard *Drosophila* medium for four generations and then moved to a 'semi-natural' medium prepared with fresh cladodes of the cactus *Opuntia ficus indica* for one generation (see Iglesias et al., 2018b for more details). This cactus species represents the more widespread host used by *D. buzzatii* in the study area. Thus, our design controlled for the known effects of age (see below), larval density, temperature, and developmental diet quality on wing morphology in *Drosophila* (Carreira et al., 2006; Loeschcke et al., 1999; Thomas, 1993).

We removed the right-wing of three to five 5-day-old flies that emerged per sex and line, and they were mounted on glass microscope slides for image acquisition. Following Muñoz-Muñoz et al. (2016) and Klingenberg (2009), a set of 15 landmarks (Fig. 1) was digitized in each wing using the TPSdig software (Rohlf, 2001). Shape information was obtained from the configurations of landmarks using standard geometric morphometrics methods as implemented in the *Geomorph* package v3.0.7 (Adams et al., 2018). We performed a principal component (PC) analysis on the whole dataset based on the covariance matrix of Procrustes residuals and used the leading 26 non-zero axes of variation in the downstream analyses.

Group differentiation

To test for population divergence and sexual dimorphism, we used a non-parametric Multivariate Analysis of Variance (npMANOVA) based on the Randomized Residuals in a Permutation Procedure (RRPP, Collyer & Adams, 2019). We tested for population, sex, and their interaction on the 26 PCs using 10,000 permutations. To evaluate which populations were sexually dimorphic, we conducted a npMANOVA for sex differences in each population individually.

Genetic and population divergence matrices estimates

We estimated the posterior distribution of the among-Line (L) and the among-Population (D) matrices by using a Bayesian multivariate mixed model implemented in the R package *MCMCglmm* (Hadfield, 2019). Population was included as a fixed factor since our conclusions are restricted to these specific populations. Line was included as a random factor nested within Population. The phenotypic data were scaled to have variance = 1 to improve estimation. We used weak non-informative priors, specifying a small degree of belief parameter (nu) of 0.002/0.001, and an average heritability of 0.5 (Berger et al., 2013; David

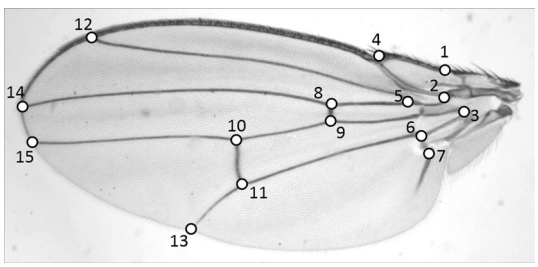

Fig. 1 Digitized landmarks in the *D. buzzatii* wing

et al., 2005). The analysis was run for 10^5 generations with 5×10^2 generations of burn-in, after which we extracted 500 samples. Convergence was verified using trace plots for all parameters. The resulting posterior distribution was then transformed to restore the original scale.

We assumed that variances and covariances of the G matrix of the inbred lines shrink by a constant proportion due to genetic drift in relation to the wild outbred populations (i.e., matrix shape is conserved, but not matrix size; Phillips et al., 2001). Thus, L can be used as a surrogate of G in examinations of the distribution of genetic covariances (i.e., cross-sex covariances). Nevertheless, the G matrix size (i.e., the proportional change in the elements of G) is particularly relevant, for instance, for detecting selection signals. Accordingly, to properly assess selection analyses (see below), we scaled the L matrix to obtain the G matrix in the base population. Inbreeding decreases the amount of additive genetic variance within lines and increases the amount of the additive genetic variance among lines (Wright, 1949). Thus, the G matrix in our study can be estimated as 1/2F of the L matrix**,** with F being the inbreeding coefficient (Wright, 1949; Falconer, 1996; Lynch & Walsh, 1998; Phillips et al., 2001). Due to the high female promiscuity in *D. buzzatii* (≅4 fathers per brood [=clutch]; Hurtado et al., 2013) and that we maintain high within-line population sizes, the inbreeding coefficient F in the isofemale lines of this study, after five generations of inbreeding, can be estimated to vary between a half-sib and a full-sib design at the moment of fly measurements. Since a smaller F means a bigger constant to scale the L matrix, we consider the F of a half-sib design to be conservative, and we multiply the L matrix by four to obtain the G matrix that we used in selection analyses. Our study also assumes the absence of dominance and interaction variance; therefore, conclusions must be drawn with the caution inherent to the isofemale line approach (David et al., 2005). Finally, the covariance matrix for the population averages was considered as the among-Population (D) matrix.

Each sex-trait combination was treated as a different trait (Sztepanacz & Houle, 2019), resulting in 52 traits. Thus, G and D are composed of four submatrices representing both patterns of integration and divergence between and within sexes as follows

$$X = \begin{bmatrix} X_m X_{mf}^t \\ X_{mf} X_f \end{bmatrix}$$

where X is the full covariance matrix, X_m and X_f are the male and female specific covariance submatrices, and X_{mf} and X_{mf}^t are the between-sex covariance submatrices, with t denoting a transpose. For G, the X_{mf} submatrix is also called B, and encodes the covariance between sexes.

Since all matrices were calculated on the PC morphospace, we back-projected the posterior matrices on the original image space to obtain the landmark variation associated with G and D. The covariance matrix Z on the original space can be obtained as follows $Z = VXV^t$ where X is either G or D calculated on the 26 non-zero PCs and V is a matrix of the 26 non-zero eigenvectors of the full covariance matrix estimated on the landmark coordinate space.

Cross-sex (co)variances and the response to selection

The diagonal elements of the B submatrix are the between-sex genetic covariance for the same trait. To investigate the magnitude of intersexual correlations (r_{mf}) in *D. buzzatii*, we standardized as a correlation each covariance. Thus, the magnitude of correlation could vary between zero, one, and minus one meaning that selection on a given trait in one sex should have no impact or result in a positive or negative correlated response, respectively, on that trait in the other sex.

We investigated how cross-sex genetic covariances may constrain or facilitate the response to selection by combining the multivariate breeder's equation, the random skewers method, and the R metric (Sztepanacz & Houle, 2019). The multivariate breeder's equation (Lande, 1979) can be written to include differences in selection and inheritance in the two sexes as follows:

$$\begin{bmatrix} \Delta\bar{z}_m \\ \Delta\bar{z}_f \end{bmatrix} = \frac{1}{2} \begin{bmatrix} G_m B^t \\ B G_f \end{bmatrix} \begin{bmatrix} \beta_m \\ \beta_f \end{bmatrix} \quad (1)$$

where $\Delta\bar{z}$ and β are the selection responses and gradients in males (m) and females (f). By generating a large number of random selection gradients and applying them to our G estimates, we can evaluate how those populations will evolve under natural selection (Cheverud & Marroig, 2007). To investigate the constraining effect of between-sexes covariances (B), one can confront the magnitude of evolution (the norm of $\Delta\bar{z}$) between a G with and without between sex covariances (B is set to a matrix of zeroes; Sztepanacz & Houle, 2019). If the ratio between both magnitudes (the R metric) is less than one, then cross-sex genetic covariances can constrain the response to selection. In contrast, $R > 1$ suggests they facilitate the response to selection. We calculated R by drawing a vector from a spherical multivariate normal distribution and applying it to a randomly drawn G matrix from our posterior distribution. This was performed 1000 times, producing a distribution of null Rs. Complementarily, we also calculated the R metric for the empirical divergence between populations. We did that by rearranging Eq. 1 to estimate β s from $\Delta\bar{z}$ drawn from our posterior distribution of fixed effects. These empirically derived β s

were then used to calculate a distribution of empirical R values as above.

Selection analysis

Finally, to detect signals of selection in the wings of females and males, we calculated the S-statistic of Ovaskainen et al. (2011). This statistical framework confronts the observed distribution of population phenotypic averages against the expected neutral divergence based on information from neutral molecular marker data. Thus, the S-statistic measures the overall evidence for selection across populations: values below 0.05 indicate strong evidence for stabilizing selection, values near 0.5 imply drift, and values above 0.95 indicate strong evidence for divergent selection (Ovaskainen et al., 2011; Karhunen et al., 2014).

In addition to a posterior sample of Gs, the Ovaskainen method requires estimating the coancestry coefficient matrix (θ) (i.e., drift distances which has a similar interpretation as the coefficient of fixation F_{ST}) between all pairs of populations. Here, we estimated θ from variation in microsatellite markers assuming an admixture F-model (AFM) and using a Metropolis–Hastings algorithm implemented in the R package RAFM (Karhunen & Ovaskainen, 2012). We analyzed data from eight microsatellite markers previously genotyped (Iglesias et al., 2018b) for 10^6 generations with a 50% burn-in, resulting in 500 posterior distribution samples. We used weak priors implemented as the default settings (Karhunen et al., 2014). To account for our experimental design, we compared F_{ST} values obtained from RAFM with F_{ST} values obtained using the isofemale line method implemented in the software Microsatellite Analyser v.4.05 (MSA; Dieringer & Schlötterer, 2003). Since we obtained higher F_{ST} values with RAFM analysis, we used both coefficients θ and F_{ST} from RAFM in selection analyses to be more conservative. We extracted the S-statistic for all 500 samples of the posterior by randomly pairing Gs and θ samples and used the average value as a global measure of selection (Ovaskainen et al., 2011). This analysis was done on both the full G and the G of each sex separately.

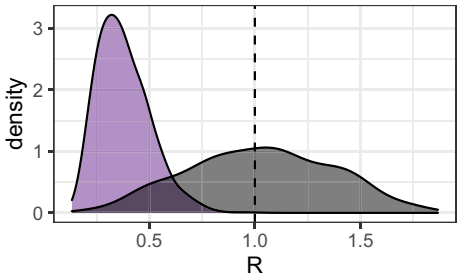

Fig. 2 The R metric of random (gray distribution) and empirically informed (purple distribution) selection gradients. Dashed line indicates R = 1, in which there is no constraining effect of between-sexes correlation

To describe the phenotypic changes potentially associated with the evidence of selection from the S-statistic, we employed the multivariate generalization of the Q_{ST}–F_{ST} test called $F_{ST}q$–F_{ST} (Chenoweth & Blows, 2008). $F_{ST}q$ is a matrix transformation analogous to the calculation of the univariate Q_{ST} and can be obtained as follows:

$$\boldsymbol{F}_{ST}q = [\boldsymbol{D} + 2\boldsymbol{G}]^{-1/2}\boldsymbol{D}[\boldsymbol{D} + 2\boldsymbol{G}]^{-1/2} \quad (2)$$

The eigenvectors of $F_{ST}q$ correspond to the directions of more or less evolutionary divergence and the eigenvalues (λ_i) are the $F_{ST}q$ for each direction. The above operation was performed on all posterior samples, resulting in a distribution of 500 $F_{ST}q$s.

On classical $F_{ST}q$–F_{ST} analyses, the eigenvalues, or Q_{ST}, for each direction are confronted against the F_{ST} calculated from neutral markers. Eigenvalues above F_{ST} suggest that the direction is under selection and values below F_{ST} suggest that the direction is under stabilizing selection (Chenoweth & Blows, 2008). However, this method ignores the possibility of differential coancestry between populations. To account for that, we used θ, and simulated 10,000 rounds of the multivariate evolution among populations (Ovaskainen et al., 2011), producing a distribution of $F_{ST}q$ for the null hypothesis of drift. The average eigenvalue of the random distribution was taken as a criterion to investigate if each

Table 1 Non-parametric Multivariate Analysis of Variance for the effect of population, sex, and their interaction on wing shape

	Df	SS	MS	R^2	F	p-value
Population	11	0.038	0.003	0.055	7.747	1E-04
Sex	1	0.009	0.009	0.013	19.953	1E-04
Population:Sex	11	0.011	0.001	0.016	2.240	1E-04
Residuals	1414	0.638	0.000	0.916		
Total	1437	0.696				

Df degrees of freedom, *SS* sum of squares, *MS* mean squares, R^2 coefficient of determination, *F* pseudo-F statistic

p-value the probability of the observed F given a null distribution based on 10,000 permutations

direction was under directional or stabilizing selection (Chenoweth & Blows, 2008).

To visualize which population or populations might be driving the results of the selection analyses, we projected the posterior distribution of phenotypic averages onto the $F_{ST}q$ space. We then visualized the expected amount of divergence by drift by projecting the posterior distribution of Gs onto the $F_{ST}q$ space and by multiplying it by $2\theta_n$ (Ovaskainen et al., 2011), where θ_n is the expected θ produced by the simulations. Shape changes associated with each $F_{ST}q$ eigenvector were obtained by getting scores ± 6 units along each axis and back-projecting those scores into the figure space. We then computed local deformations (Marquez et al., 2012) to identify which regions of the wing were compressing or expanding. This procedure produced four wing shapes per axis: a male and a female shape for negative and positive values.

To evaluate if the sexes were evolving in a similar direction along each $F_{ST}q$ axis, we calculated the vector correlation between the shape changes associated with each sex for each axis. When sexes evolve in the same direction we expected positive values, near to one, but we expected negative values, near to − 1 when sexes evolve in opposite directions. These calculations were done over the entire posterior, but for simplicity, we show the projection of all the samples onto the mean $F_{ST}q$, which summarizes the main directions of selection over the entire posterior.

Finally, to quantify the association between the intensity of selection and the evolution of dimorphism we calculated the Spearman's Rank Correlation Coefficient between each axis-specific $F_{ST}q$ value (intensity of selection) and the between-sex vector correlation (evolution of dimorphism).

Both driftsel, $F_{ST}q$–F_{ST} and multivariate simulations are implemented in the R package emorph2 (https://github.com/FabioLugar/emorph2). These analyses were done both for the full dataset, which includes the phenotype of both sexes, but also were performed for each sex alone. However, it is important to highlight that analyzing the sexes separately ignores the possibility of intralocus sexual conflict, and, thus, was used only as a baseline comparison of the relative intensity of selection on both sexes.

Results

Group differentiation- Populations and sexes are different, but differences are small

The npMANOVA testing for the difference among populations, between sexes, and their interaction on wing shape showed that all factors are significant (Table 1). All these effects account for ~ 8.5% of the total variation, although Population alone explained more than half of it. When sexual dimorphism was investigated for each population individually, all tests were significant (p-value < 0.03 in all cases), with one exception (population MG, p-value = 0.116). The removal of this population from subsequent analyses did not alter the results presented here, so we present the analysis using all 12 populations for simplicity.

Cross-sex (co)variances and the response to selection

The 95% highest-density intervals for the intersexual correlations (r_{mf}) of the posterior distributions of B ranged from 0.33 to 0.88, suggesting a low to a high degree of between-sex pleiotropy on wing traits (Figure S1).

We quantified the net effect of cross-sex covariances by calculating the R metric using both simulated random selection gradients and empirically informed β s for the sexual divergence observed between populations. The R metric based on simulated random selection gradients shows a distribution centered at one, that spreads evenly towards high and low values (Fig. 2). This suggests that cross-sex covariances can either constrain or facilitate the evolution of *D. buzzattii* wing. On the other hand, the R values calculated based on empirically informed β s show a highly skewed distribution to lower values (Fig. 2), indicating that the observed populational differences occurred along constrained directions.

Selection analysis- signal of divergent selection on wing shape in females and males

For the analyses of both female and male phenotypes jointly, the S-statistic recovered a strong signal of directional selection (mean S = 1). For the $F_{ST}q$–F_{ST} analysis, the use of the driftsel framework to produce a neutrality expectation (i.e., null $F_{ST}q$) produced values that were lower than the ones obtained for the F_{ST} coefficient. Nevertheless, irrespective of the criteria used, at least four axes of the analysis of both sexes had 95% credibility intervals above the neutrality expectations, suggesting the action of directional selection (Fig. 3).

The projection of the posterior sample of population phenotypic averages on the four leading $F_{ST}q$ axes shows that eight of the 12 populations diverged more than the expected under drift (Fig. 4). The visualization of the shape changes associated with these axes reveals that both sexes are selected toward differing phenotypes (Fig. 4). For the first $F_{ST}q$ axis, the females vary from thinner to larger base wings, while males vary from smaller to larger blade wings. For the second axis, both males and females vary in the same direction from thinner to thicker wings, but substantial variation is observed between the sexes in internal landmarks. For the third axis, the overall shape changes are conflicting,

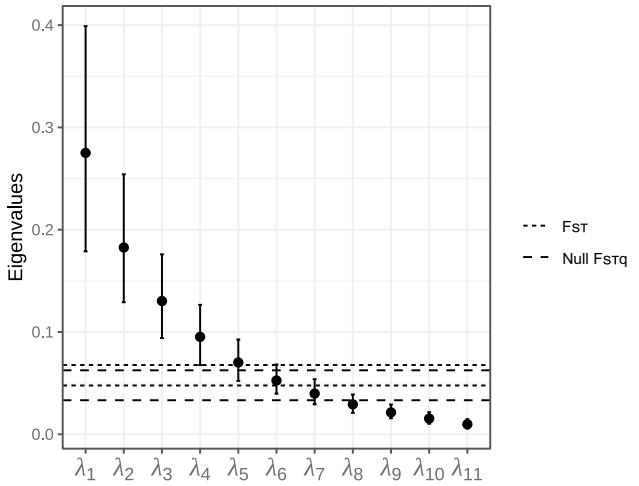

Fig. 3 Distribution of eigenvalues of the posterior sample for the $F_{ST}q$ analysis for the full analysis, including female and male phenotypes. Dots are mean values, and error bars are the 95% highest density intervals. Horizontal lines represent the interval for the differentiation expected under random genetic drift scaling according to the driftsel analysis (null $F_{ST}q$) and according to F_{ST} from RAFM

with males' wings on one extreme of the axis being similar to females 'wings on the opposite extreme of the axis. For the fourth axis, the variation described for both sexes is very similar, with an overall distinction between thinner and larger wings.

The vector correlations between sex-specific shape changes reinforce this idea that the sexes are diverging along the major $F_{ST}q$ axes, but evolve more aligned along the axes that are not under directional selection (Fig. 5). Specifically, the stronger the signal of directional selection ($F_{ST}q$), the lowest the vector correlation between the sexes (Fig. 5A). This is also reflected in the negative coefficients of the Spearman correlations among $F_{ST}q$ values and between-sex vector correlations (median = − 0.65; Fig. 5B).

When sexes were analyzed independently, we also found a strong signal of selection for both sexes (females mean S = 0.973, males mean S = 0.978). $F_{ST}q$ analyses show that for males three axes were above the expected under drift, while for females, only two (Figure S2). Additionally, males presented $F_{ST}q$ values that were on average higher than the ones for females, suggesting that selection is more intense for this sex (Figure S2).

The pattern of phenotypic differentiation in selected traits when each sex was analyzed separately is shown in Figure S3. Shape deformations summarized for each sex (Figure S4) were somewhat similar to the ones for the analysis of both phenotypes combined. For females, the first and second axes are more strongly aligned with the second and first axes of the global analysis (axis correlation of 0.88 and 0.74, respectively). For males, the first and second axes are more strongly aligned with the first and fourth axes of the global

Fig. 4 Projection of the posterior distribution of the population phenotypic averages onto the $F_{ST}q$ space formed by the first and second axes (**A**) and by the third and fourth axes (**B**). Transparent dots represent individual samples of the posterior and solid dots are the averages. Circles represent the expected divergence under drift. Wings represent changes along the axes for both females and males. Colors represent local deformation values indicating expansions (red) and contractions (blue). Deformations were multiplied by 6 standard deviations to help the visualization (Color figure online)

analysis (axis correlation 0.91 and 0.77, respectively). The third axis of the male-specific $F_{ST}q$ aligned moderately with the fourth axis of the combined $F_{ST}q$ as well (axis correlation of 0.58). Because most results of the separate sexes are contemplated by the combined analysis and because we found a significant empirical effect of cross-sex covariances (Fig. 2), we here focus mainly on the results of the combined analyses.

Discussion

We examined wing morphological changes in *D. buzzatii* in terms of evolutionary constraints and opportunities of its G matrix. We emphasize two findings. First, we showed that G can facilitate or constrain the evolution of *D. buzzatii* wings. However, we found that wing evolution is actually happening in directions constrained by G, resulting in low sexual dimorphism, and highlighting the restrictive role of between-sex pleiotropy in the evolution of sexual shape dimorphism. Second, our results suggest that the wings of females and males are under different selection strengths, being more intense and with more selected dimensions in males.

The driftsel and multivariate Q_{ST} analyses ($F_{ST}q$) showed a clear signal of directional selection on wing shape (Fig. 3), and that divergence was mostly concentrated on males rather than females (Figure S2). The leading eigenvectors of $F_{ST}q$, which are the axes of morphological variation most affected by directional selection, indicated that the major axes of divergence were not in the same direction for each sex (Fig. 5) and suggest that males and females have a somewhat independent evolutionary history. The $F_{ST}q$ analyses of each sex separately revealed three morphological axes under directional selection in males, but only two axes in females (Figure S2). This asymmetry suggests a wider array of functional demands on male wings than on females, which agrees with the double function of wings in males, like flight and courtship song production. Iglesias et al. (2018b) showed that males of these same sampled populations have divergent courtship songs, which they produce with their wings. These authors found evidence consistent with the role of directional selection in the divergence of courtship song traits, which could be associated with wing shape changes shown

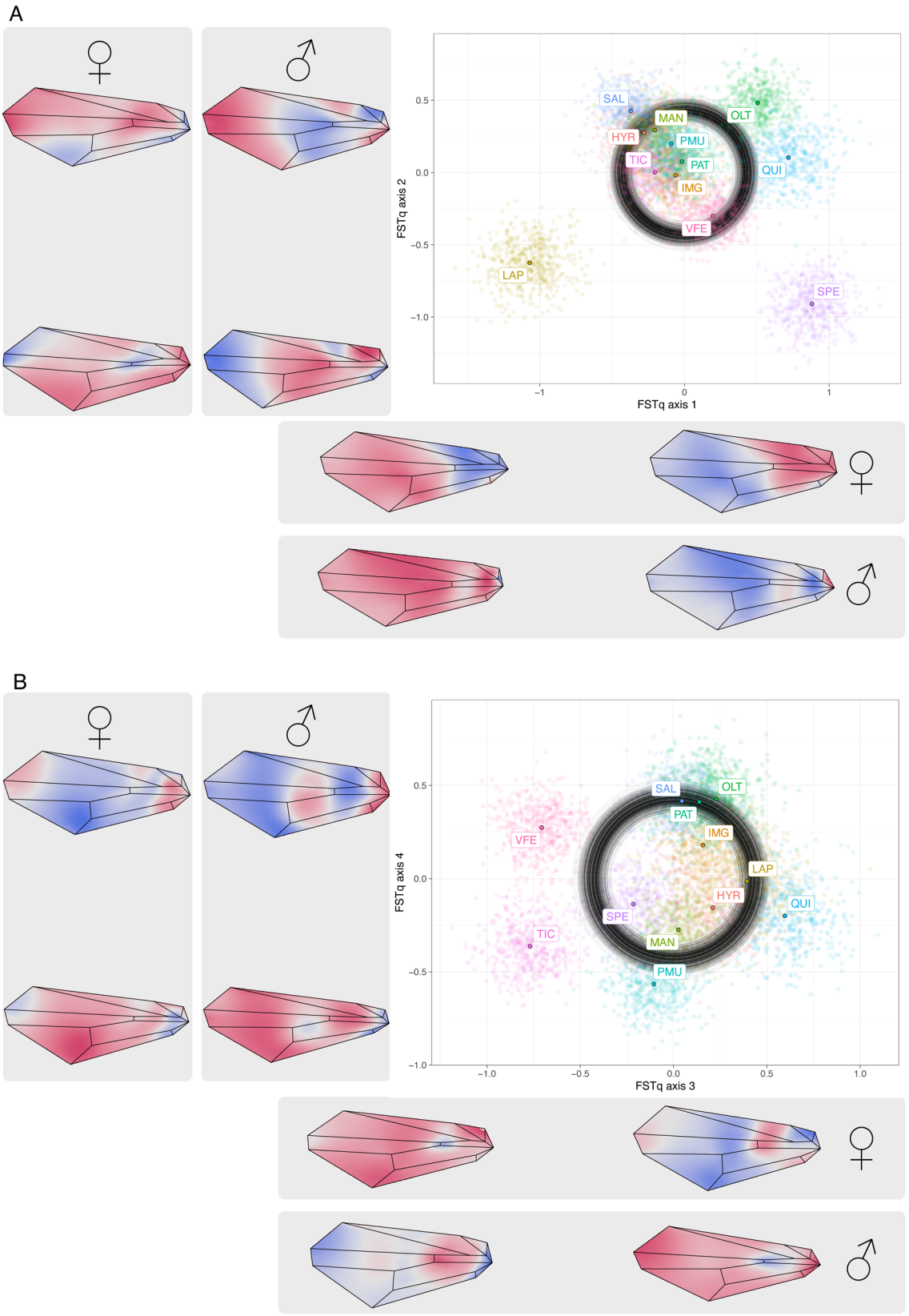
A
SAL
MAN
OLT
HYR
PMU
TIC
PAT
QUI
IMG
VFE
LAP
SPE
FSTq axis 2
FSTq axis 1
B
SAL
OLT
PAT
IMG
VFE
LAP
HYR
QUI
SPE
TIC
MAN
PMU
FSTq axis 4
FSTq axis 3

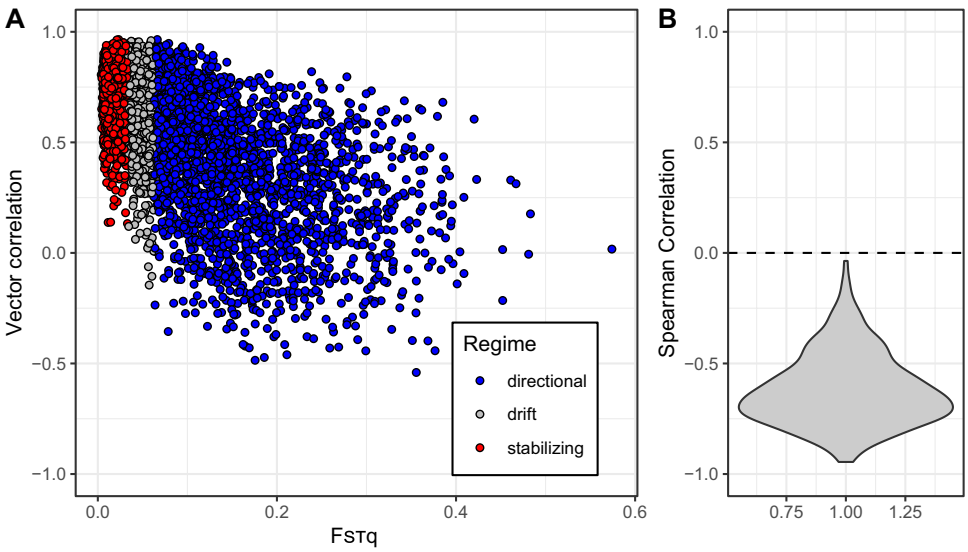

Fig. 5 **A** Relationship between the axis-specific $F_{ST}q$ and between-sex vector correlations for all eigenvectors obtained from the posterior distribution. **B** Spearman correlation coefficient obtained for the relationship between Q_{ST} and among-sex vector correlations for each sample. The dashed line represents the zero correlation

here. Although the methodology is different in both works, the OLT population, and SPE to a lesser degree, showed differentiation in both song parameters and male wing shape (Fig. 3 in Iglesias et al., 2018b and Figures S3 in this work). This potential male-specific selection on the wing for song production could also explain the asymmetry found in the number of axes under selection between male and female *D. buzzatii*.

We found that cross-sex covariances reduced the predicted response to selection in the direction of the extant sexual dimorphism, in line with previous results in *D. melanogaster's* wing (Abbott et al., 2010; Sztepanacz & Houle, 2019). Thus, it is possible that selection along constrained directions had to be intensified to circumvent the limitations imposed by G (Machado, 2020). However, while in *D. melanogaster* the predicted response to selection in random directions is also reduced, in *D. buzzatii* responses can be either reduced or augmented. This discrepancy may reflect the more variable intersexual correlations (r_{mf}) found in the wing of *D. buzzatii* (r_{mf} = 0.33–0.88) relative to values observed in *D. melanogaster's* wing (r_{mf} = 0.907–0.940; Sztepanacz & Houle, 2019). In the brightly colored dewlap of Anolis lizards, for example, r_{mf} values were lower (r_{mf} = 0.39–0.41), and cross-sex covariances (B) had little effect on the predicted response to selection either in random directions and in the direction of sexual dimorphism (Cox et al., 2017). Thus, our results reinforce the idea that the intensity of correlations determines if populations will be constrained or not by B.

The theory states that sexually antagonistic selection will favor a reduction in cross-sex genetic covariance when the strength of selection is highly asymmetric between the sexes (McGlothlin et al., 2019). Otherwise, sexually antagonistic selection will tend to maintain strong cross-sex genetic covariance when the strength of selection is similar in each sex (McGlothlin et al., 2019). If that holds for the populations investigated here, the variable r_{mf} values observed in *D. buzzatii* may result from different intensities of sex-specific selection in the different linear trait combinations. In addition to the potential male-specific selection on the wing for song production, natural selection for aerodynamics could also produce between-sex coordinated and uncoordinated evolution. Wing shape is known to affect flight performance in *Drosophila* (Chin & Lentink, 2016; Ray et al., 2016), and males are known to be the more dispersive sex in various species (Begon, 1976; Fontdevila & Carson, 1978; Markow & Castrezana, 2000; Mishra et al., 2020; Powell et al., 1976). Sex bias in dispersal is affected by many factors and interactions such as predispersal context, mate shortage, and availability of resources, which might vary among populations and exert different selective pressures (Mishra et al., 2018; Tung et al., 2018).

In short, the evolution of *D. buzzatii* wing shape seems to be the product of a complex interplay between the genetic constraints due to between-sex pleiotropy, and conflicting sexual and natural selections. Future studies on the causal links between wing morphology, song production, and aerodynamics of *D. buzzatii* are needed to provide a better picture of how cross-sex covariances can indirectly evolve as a by-product of selection on mating success and biomechanical performance.

Supplementary Information The online version contains supplementary material available at https://doi.org/10.1007/s11692-022-09593-x.

Acknowledgements We sincerely thank Gladys Hermida for allowing access to its laboratory facilities to produce the photographs used in this study, Victoria Garcia for helpful discussions that helped improve previous versions of this manuscript, and Diogo Melo for his help with the G matrix estimation. We also thank Consejo Nacional de Investigaciones Científicas y Técnicas (CONICET), ANPCyT (PICT 2013-1121 and PICT-2019-2557) and NSF (DEB 1350474 and DEB 1942717) for

financial support. Finally, we would like to thank Dr. David Houle for their constructive comments and suggestions that greatly improved this work.

Author contributions PPI, FAM and EMS conceived the project, EH supervised the global project in which the present work is embedded and contributed materials and reagents; EMS performed wing dissections, SL took the photographs, PPI and FAM conducted analyses, PPI and FAM wrote the original draft, which was discussed, edited and revised by all authors.

Data Availability Data and scripts used in this work are available at https://github.com/FabioLugar/Dbuzzatii.

Declarations

Conflict of interest The author declares no conflict of interest.

References

Abbott, J. K., Bedhomme, S., & Chippindale, A. K. (2010). Sexual conflict in wing size and shape in *Drosophila melanogaster*. *Journal of Evolutionary Biology, 23*(9), 1989–1997.

Adams, D. C., Collyer, M. L., Kaliontzopoulou, A., & Sherratt, E. (2018). Geomorph: Software for geometric morphometric analyses. *R Package, 3*, 4.

Arnold, S. J. (1992). Constraints on phenotypic evolution. *The American Naturalist, 140*, S85–S107.

Begon, M. (1976). Dispersal, density and microdistribution in *Drosophila subobscura* Collin. *The Journal of Animal Ecology, 45*, 441–456.

Berger, D., Postma, E., Blanckenhorn, W. U., & Walters, R. J. (2013). Quantitative genetic divergence and standing genetic (co) variance in thermal reaction norms along latitude. *Evolution, 67*(8), 2385–2399.

Blows, M., & Walsh, B. (2009). Spherical cows grazing in flatland: Constraints to selection and adaptation. *Adaptation and fitness in animal populations* (pp. 83–101). Dordrecht: Springer.

Bürger, R., & Lynch, M. (1995). Evolution and extinction in a changing environment: A quantitative-genetic analysis. *Evolution, 49*(1), 151–163.

Carreira, V. P., Soto, I. M., Hasson, E., & Fanara, J. J. (2006). Patterns of variation in wing morphology in the cactophilic *Drosophila buzzatii* and its sibling *D. koepferae*. *Journal of Evolutionary Biology, 19*(4), 1275–1282.

Chenoweth, S. F., & Blows, M. W. (2008). Q_{ST} meets the G matrix: The dimensionality of adaptive divergence in multiple correlated quantitative traits. *Evolution, 62*(6), 1437–1449.

Cheverud, J. M., & Marroig, G. (2007). Comparing covariance matrices: random skewers method compared to the common principal components model. *Genetics and Molecular Biology, 30*, 461–469.

Chevin, L. M., Lande, R., & Mace, G. M. (2010). Adaptation, plasticity, and extinction in a changing environment: Towards a predictive theory. *PLoS Biology, 8*(4), e1000357.

Chin, D. D., & Lentink, D. (2016). Flapping wing aerodynamics: From insects to vertebrates. *Journal of Experimental Biology, 219*(7), 920–932.

Collyer, M. L., & Adams, D. C. (2019). RRPP: linear model evaluation with randomized residuals in a permutation procedure. *R package version* 0.4. 0.[WWW Document]. https://cran.r-project.org/package=RRPP

Cox, R. M., Costello, R. A., Camber, B. E., & McGlothlin, J. W. (2017). Multivariate genetic architecture of the Anolis dewlap reveals both shared and sex-specific features of a sexually dimorphic ornament. *Journal of Evolutionary Biology, 30*(7), 1262–1275.

David, J. R., Gibert, P., Legout, H., Pétavy, G., Capy, P., & Moreteau, B. (2005). Isofemale lines in Drosophila: An empirical approach to quantitative trait analysis in natural populations. *Heredity, 94*(1), 3–12.

Dieringer, D., & Schlötterer, C. (2003). Microsatellite analyzer (MSA): A platform independent analysis tool for large microsatellite data sets. *Molecular Ecology Notes, 3*(1), 167–169.

Falconer, D. S. (1996). *Introduction to quantitative genetics*. Pearson Education.

Fontdevila, A., & Carson, H. (1978). Spatial distribution and dispersal in a population of *Drosophila*. *The American Naturalist, 112*, 365–394.

Futuyma, D. J. (2010). Evolutionary constraint and ecological consequences. *Evolution International Journal of Organic Evolution, 64*(7), 1865–1884.

Hadfield, J. (2019). Package MCMCglmm.

Houle, D., & Meyer, K. (2015). Estimating sampling error of evolutionary statistics based on genetic covariance matrices using maximum likelihood. *Journal of Evolutionary Biology, 28*(8), 1542–1549.

Hurtado, J., Iglesias, P. P., Lipko, P., & Hasson, E. (2013). Multiple paternity and sperm competition in the sibling species *Drosophila buzzatii* and *Drosophila koepferae*. *Molecular Ecology, 22*(19), 5016–5026.

Iglesias, P. P., & Hasson, E. (2017). The role of courtship song in female mate choice in South American Cactophilic *Drosophila*. *PLoS ONE, 12*(5), e0176119.

Iglesias, P. P., Soto, E. M., Soto, I. M., Colines, B., & Hasson, E. (2018a). The influence of developmental environment on courtship song in cactophilic *Drosophila*. *Journal of Evolutionary Biology, 31*(7), 957–967.

Iglesias, P. P., Soto, I. M., Soto, E. M., Calderón, L., Hurtado, J., & Hasson, E. (2018b). Rapid divergence of courtship song in the face of neutral genetic homogeneity in the cactophilic fly *Drosophila buzzatii*. *Biological Journal of the Linnean Society, 125*(2), 321–332.

Karhunen, M., & Ovaskainen, O. (2012). Estimating population-level coancestry coefficients by an admixture F model. *Genetics, 192*(2), 609–617.

Karhunen, M., Ovaskainen, O., Herczeg, G., & Merilä, J. (2014). Bringing habitat information into statistical tests of local adaptation in quantitative traits: A case study of nine-spined sticklebacks. *Evolution, 68*(2), 559–568.

Klingenberg, C. P. (2009). Morphometric integration and modularity in configurations of landmarks: Tools for evaluating a priori hypotheses. *Evolution & Development, 11*(4), 405–421.

Lande, R. (1979). Quantitative genetic analysis of multivariate evolution applied to brain: Body size allometry. *Evolution, 33*, 402–416.

Lande, R. (1993). Risks of population extinction from demographic and environmental stochasticity and random catastrophes. *The American Naturalist, 142*(6), 911–927.

Loeschcke, V., Bundgaard, J., & Barker, J. S. F. (1999). Reaction norms across and genetic parameters at different temperatures for thorax and wing size traits in *Drosophila aldrichi* and *D. buzzatii*. *Journal of Evolutionary Biology, 12*(3), 605–623.

Lynch, M., & Walsh, B. (1998). *Genetics and analysis of quantitative traits*. Sinauer.

Machado, F. A. (2020). Selection and Constraints in the ecomorphological adaptive evolution of the skull of living Canidae (Carnivora, Mammalia). *The American Naturalist, 196*(2), 197–215.

Markow, T. A., & Castrezana, S. (2000). Dispersal in cactophilic *Drosophila*. *Oikos, 89*(2), 378–386.

Márquez, E. J., Cabeen, R., Woods, R. P., & Houle, D. (2012). The measurement of local variation in shape. *Evolutionary Biology, 39*(3), 419–439.

McGlothlin, J. W., Cox, R. M., & Brodie, E. D., III. (2019). Sex-specific selection and the evolution of between-sex genetic covariance. *Journal of Heredity, 110*(4), 422–432.

Mishra, A., Tung, S., Shree Sruti, V. R., Srivathsa, S., & Dey, S. (2020). Mate-finding dispersal reduces local mate limitation and sex bias in dispersal. *Journal of Animal Ecology, 89*(9), 2089–2098.

Mishra, A., Tung, S., Sruti, V. S., Sadiq, M. A., Srivathsa, S., & Dey, S. (2018). Pre-dispersal context and presence of opposite sex modulate density dependence and sex bias of dispersal. *Oikos, 127*(11), 1596–1604.

Muñoz-Muñoz, F., Carreira, V. P., Martínez-Abadías, N., Ortiz, V., González-José, R., & Soto, I. M. (2016). *Drosophila* wing modularity revisited through a quantitative genetic approach. *Evolution*, *70*(7), 1530−1541.

Ovaskainen, O., Karhunen, M., Zheng, C., Arias, J. M. C., & Merilä, J. (2011). A new method to uncover signatures of divergent and stabilizing selection in quantitative traits. *Genetics*, *189*(2), 621–632.

Phillips, P. C., Whitlock, M. C., & Fowler, K. (2001). Inbreeding changes the shape of the genetic covariance matrix in *Drosophila melanogaster*. *Genetics, 158*(3), 1137–1145.

Powell, J. R., Dobzhansky, Th., Hook, J. E., & Wistrand, H. (1976). Genetics of natural populations. XLIII. Further studies on rates of dispersal of *D. pseudoobscura* and its relatives. *Genetics, 82*, 495–506.

Ray, R. P., Nakata, T., Henningsson, P., & Bomphrey, R. J. (2016). Enhanced flight performance by genetic manipulation of wing shape in *Drosophila*. *Nature Communications, 7*(1), 1–8.

Rohlf, F. J. (2001). Tps Dig v. 1.28. Free computer software for collecting landmark data from images. *Ecology and Evolution*, SUNY at Stony Brook. http://life.bio.sunysb.edu/morph.

Steppan, S. J., Phillips, P. C., & Houle, D. (2002). Comparative quantitative genetics: Evolution of the G matrix. *Trends in Ecology & Evolution, 17*(7), 320–327.

Sztepanacz, J. L., & Houle, D. (2019). Cross-sex genetic covariances limit the evolvability of wing-shape within and among species of *Drosophila*. *Evolution, 73*(8), 1617–1633.

Thomas, R. H. (1993). Ecology of body size in *Drosophila buzzatii*: Untangling the effects of temperature and nutrition. *Ecological Entomology, 18*(1), 84–90.

Tung, S., Mishra, A., Shreenidhi, P. M., Sadiq, M. A., Joshi, S., Sruti, V. S., & Dey, S. (2018). Simultaneous evolution of multiple dispersal components and kernel. *Oikos, 127*(1), 34–44.

Villmoare, B. (2013). Morphological integration, evolutionary constraints, and extinction: A computer simulation-based study. *Evolutionary Biology, 40*(1), 76–83.

Wright, S. (1949). The genetical structure of populations. *Annals of Eugenics, 15*(1), 323–354.